Spin Ice under Pressure: Symmetry Enhancement and Infinite Order Multicriticality

L. D. C. Jaubert,[1] J. T. Chalker,[2] P. C. W. Holdsworth,[3] and R. Moessner[1]

[1]*Max-Planck-Institut für Physik komplexer Systeme, 01187 Dresden, Germany*
[2]*Theoretical Physics, Oxford University, 1 Keble Road, Oxford, OX1 3NP, United Kingdom*
[3]*Laboratoire de Physique, École Normale Supérieure de Lyon, CNRS, 69364 Lyon Cedex 07, France*

We study the low-temperature behavior of spin ice when uniaxial pressure induces a tetragonal distortion. There is a phase transition between a Coulomb liquid and a fully magnetized phase. Unusually, it combines features of discontinuous and continuous transitions: the order parameter exhibits a jump, but this is accompanied by a divergent susceptibility and vanishing domain wall tension. All these aspects can be understood as a consequence of an emergent SU(2) symmetry at the critical point. We map out a possible experimental realization.

One fascinating aspect of condensed matter physics is the extent to which the nature and symmetries of emergent low-energy degrees of freedom can be independent of the high energy ones from which they derive. While low-energy degrees of freedom of many types are possible, systems in which these correspond to a gauge field are still rare. In this paper we study this theme in a setting which brings forth an unusual sequence of low-energy fluctuations and symmetries: we consider spin ice, a frustrated Ising magnet on the pyrochlore lattice, whose low-temperature behavior is well described by a gauge field, an emergent magnetostatics, representing a so-called Coulomb phase where correlations decay algebraically as r^{-3}. Transitions out of such a phase have attracted a great deal of attention recently [1–5].

We ask what happens when the host crystal is subjected to uniaxial pressure. This is a powerful probe which has previously produced interesting information in frustrated magnets [6,7]. Specifically, we consider a pressure-induced strain that lowers the crystal symmetry from cubic to tetragonal. We find that this induces a highly unusual symmetry-breaking phase transition out of the Coulomb phase: it is characterized by discontinuities in the magnetization and energy, without being first order. Rather, it occurs at a multicritical point of infinite order and is accompanied by a divergent susceptibility. We demonstrate both these features using Monte Carlo simulations. Further salient properties of the critical point include the absence of a domain wall tension, along with spin correlations that vanish in a plane perpendicular to the strain-induced tetragonal axis. These should be observable experimentally, and we discuss the scope for realizing such a transition in the laboratory.

The unusual nature of the transition is a consequence of an emergent SU(2) symmetry: as the pressure reduces the symmetry of the *external* space, an enhanced *internal* symmetry appears. We show this by means of an exact solution in three dimensions at the critical temperature and a mapping to a quantum phase transition in 2 + 1 dimen-

sions, between Ising and *XY* anisotropy in a spin-1/2 ferromagnet. Transitions with analogous features have been studied previously in the context of ferroelectrics [8], using versions of the model for potassium dihydrogen phosphate (KDP) introduced by Slater [9], which in its two-dimensional form is equivalent to the six-vertex model and exactly solved [10]. Spin ice has the potential to provide a much cleaner realization of this physics than the transition in ferroelectrics, since its magnetic degrees of freedom are much more accurately represented by Ising variables supported on a rigid lattice.

Spin ice is well modeled by Ising spins $\mathbf{S}_i$ parallel to their local easy axis on the pyrochlore lattice [11]. At low temperature, we can limit ourselves to the highly degenerate ground state ensemble with two spins pointing in and two out of each tetrahedron (ice rules) and consider effective nearest neighbor interactions [12,13]. After coarse graining the magnetization, the discrete ice rules can be written in terms of a continuum zero-divergence constraint from which emerges the algebraic correlations [14,15]. We lift the degeneracy underlying the Coulomb phase via the exchange modulation

$$\mathcal{H} = -\sum_{\langle i,j \rangle} J_{ij} \mathbf{S}_i \cdot \mathbf{S}_j, \tag{1}$$

where $J_{ij} = J - \delta > 0$ for bonds on (001) planes perpendicular to the strain axis, and $J_{ij} = J$ otherwise (see Fig. 1). For $\delta > 0$, the $\mathbb{Z}_2$ symmetry of this Hamiltonian is spontaneously broken at temperature $T_c \sim \delta$ in favor of a state magnetized parallel to the [001] direction. If the strain were very large, so that $T_c \sim J$, ordering would be from a conventional paramagnetic state and in the standard three-dimensional Ising universality class. In contrast, for realistic small strains, T_c is much less than J and ordering is from the Coulomb phase, with the striking features we describe.

We first present results from Monte Carlo simulations in which efficient loop updates preserve the ice rules [16,17]. The temperature dependence of the magnetization M and
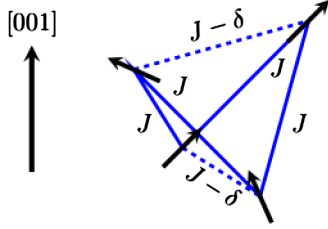
FIG. 1 (color online). A tetrahedron of the pyrochlore lattice
with exchange J and $J - \delta$ as indicated: the dashed bonds lie in
(001) planes. One of the two ground states for $\delta > 0$ is shown.

of the inverse susceptibility χ^{-1} are shown in Fig. 2, upper
panel: remarkably, M takes its saturation value M_{sat} at all
temperatures below T_c, but χ diverges as T_c is approached
from above. To better characterize the transition, we also
examine the probability distribution function (PDF) of the
order parameter; shown in Fig. 2, lower panel. This is a
standard diagnostic: two peaks are expected in the PDF at
the transition point when this is first order, but only one
peak if it is continuous [18]. Again, we find unconventional
behavior: a PDF that is uniform *over all values* of M at T_c.

An exactly uniform order parameter distribution arises
within Landau theory as a limiting case. The free energy
$G(M)$ close to a multicritical point of order n is

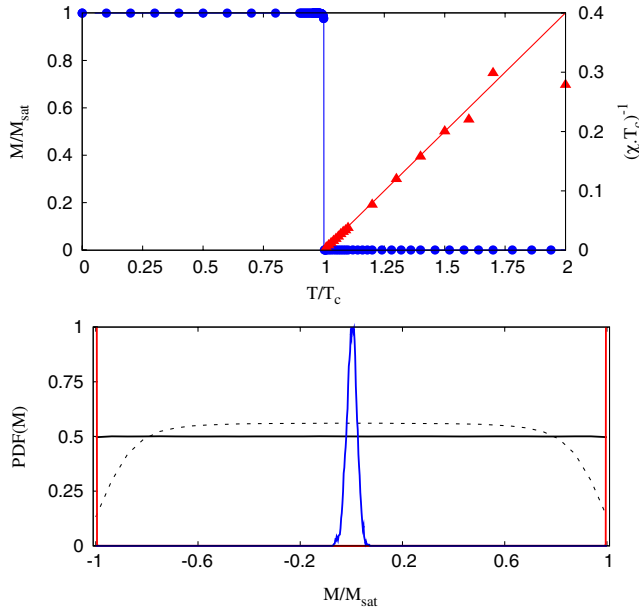$$G(M) = \frac{a}{2}(T - T_c)M^2 + \frac{b}{2n}M^{2n}. \tag{2}$$

FIG. 2 (color online). *Top*: Simulation data for M (blue circles)
and $(\chi T_c)^{-1}$ (red triangles) vs T/T_c. Bottom: PDF of M/M_{sat} at
different temperatures. For $T < T_c$ (red) the PDF has two sharp
peaks at $M = \pm M_{sat}$. For $T = T_c$ (black) the PDF is broad in
small samples (dashed black line for $L_\perp = L_z = 4$) and almost
flat in larger samples (solid black line for $L_\perp = 4$ and $L_z = 18$).
For $T > T_c$ (blue) the PDF is Gaussian. (Values at $T \neq T_c$ scaled
to fit on vertical axis.)

In the limit $n \to \infty$, it is independent of M for $|M| < 1$ at
$T = T_c$. Moreover, the order parameter exponent takes the
value $\beta = 1/(2n - 2)$, generating a jump for $n \to \infty$.
Also, the susceptibility ($\chi \sim A_\pm |(T - T_c)/T_c|^{-\gamma}$ for $T \gtrless$
T_c) has an exponent $\gamma = 1$ independent of n and an am-
plitude ratio $A_-/A_+ = 1/(2n - 2)$ that vanishes as $n \to$
∞. All these are features of our simulations. This success
of mean field theory reflects the exceptional value of the
upper critical dimension, $d_{c2} = 1$, which follows from
standard arguments with allowance for the anisotropic
spatial scaling; see Eq. (5) below. This symmetry-breaking
transition differs markedly from the symmetry-sustaining
Kasteleyn transition induced in the same system at $\delta = 0$
by an applied field [5].

In previous discussions of the ferroelectric KDP model
[8–10,19–22] some distinctive aspects have been recog-
nized. Indeed, Slater's original approximation [9] yields a
free energy independent of the order parameter at the
transition, which on this basis has been called infinite order
[23]. Such a conclusion is evidently very delicate [19], and
corrections to the approximation or physical perturbations
have the potential to convert the transition into a conven-
tional one: either first order or continuous. This is in fact
the case for the material KDP itself, which has a first-order
transition that can be driven through a tricritical point
under pressure [8]. While in two dimensions an exact
solution of the KDP model corroborates the main features
of Slater's results [10,22,24], it is not *a priori* clear what
this tells us for higher dimension.

The ice rules impose the same value of the magnetiza-
tion M in all (001) planes: any configuration can be
mapped onto an ensemble of strings of down spins span-
ning the system from top to bottom, with the convention
that the string vacuum is the state in which all spins are up
[19]. The number of strings defines (i) the total magneti-
zation and (ii) a topological sector, so that the former can
be used to label the latter. The equiprobability of all sectors
(see Fig. 2) already suggests that the free energy is inde-
pendent of the number of strings. This observation can be
made precise using the transfer matrix that acts between
two adjacent (001) layers of the lattice [25]. Since this
transfer matrix is a direct product of factors **T** representing
separate tetrahedra, we first discuss a single tetrahedron. A
single string can enter the tetrahedron at either site in one
(001) layer and leave it at either site in the other layer, with
energy cost $4\delta/3$. This sector is therefore represented in **T**
by a 2×2 block in which all entries are the Boltzmann
factor $\Gamma = e^{-4\delta\beta/3}$. By contrast, zero or two strings in a
tetrahedron cost no energy and impose the next configura-
tion locally, generating two 1×1 blocks with unit entries
in **T**. For later use, we also introduce a matrix Σ^+; these
two have the form

$$\mathbf{T} = \begin{pmatrix} 1 & & & \\ & \Gamma & \Gamma & \\ & \Gamma & \Gamma & \\ & & & 1 \end{pmatrix} \quad \text{and} \quad \Sigma^+ = \begin{pmatrix} 0 & 1 & 1 & 0 \\ 0 & 0 & 0 & 1 \\ 0 & 0 & 0 & 1 \\ 0 & 0 & 0 & 0 \end{pmatrix}. \tag{3}$$

The maximum eigenvalues of **T** lie for $T < T_c = \frac{4\delta}{3\ln 2}$ in the two fully magnetized sectors, but for $T = T_c$ all sectors have the same maximal eigenvalue. In addition, the associated eigenvector in the one-string sector is (1,1). Explicit calculation of the transfer matrix for a complete lattice is complicated by the fact that the repeat unit in the (001) direction involves four different layers. Nevertheless, its maximal eigenvalues inherit precisely the properties described for **T**, and at $T = T_c$ the associated eigenvectors in each sector give equal weight to all arrangements of strings on a (001) layer. The maximal eigenvalues determine the physical properties in the thermodynamic limit with $L_z \gg L_\perp$. As a result: (a) below T_c the magnetisation is saturated; and (b) at T_c all sectors are equiprobable and all configurations within a sector are equiprobable. (b) means that the absence of the terms M^4, $M^6 \ldots$ from Eq. (2) at the transition point is an exact feature of the model. Remarkably, both (a) and (b) continue to hold even if the four interactions labeled J in Fig. 1 differ by $\delta' < \delta$ (as happens if the strain axis is not exactly along [100]). Then the entries Γ in **T** take different values, Γ_1 and Γ_2, on and off the diagonal, but at T_c (where $\Gamma_1 + \Gamma_2 = 1$) all sectors are again degenerate.

The transfer matrix for the complete lattice can alternatively be thought of as the evolution operator in imaginary time for a two-dimensional quantum XXZ model (in analogy with Eq. (8) of [10]). The coarse-grained quantum Hamiltonian is

$$\mathcal{H}_Q = -J\sum_{\langle i,j\rangle}(s_i^x s_j^x + s_i^y s_j^y + \Delta s_i^z s_j^z). \qquad (4)$$

The strings thus denote the world lines of $s_i^z = 1/2$ spins. In this language the decomposition into sectors is a consequence of the conservation of total s^z, and is due to a U(1) symmetry. The ground state of $\mathcal{H}_Q$ has ferromagnetic order of the quantum spins for all Δ, with an orientation for the magnetization that depends on on Δ. For $\Delta < 1$, spins lie in the x-y plane and the state has zero-point fluctuations, representing the Coulomb phase. For $\Delta > 1$, spins are aligned along the z axis and the state has no fluctuations, representing the low-temperature phase of the classical system. The equiprobability of string sectors at the critical point corresponds here to the degeneracy of the $N + 1$ ground states of the isotropic Heisenberg ferromagnet with N spins, for all values of the total magnetization $\Sigma^z = \{-N/2, \ldots, N/2\}$. We have confirmed that this isotropy is a property of the full transfer matrix for the classical spin model, and not only of its leading eigenvectors or of the effective quantum description. We do this by checking that the classical transfer matrix commutes with the total spin raising operator, represented for a single tetrahedron by Σ^+, given in Eq. (3). This constitutes an enhancement of the symmetry at the critical point from U(1) to SU(2).

The quantum description can be employed to calculate correlation functions within a given sector in spin ice, by approximating the imaginary time direction as continuous
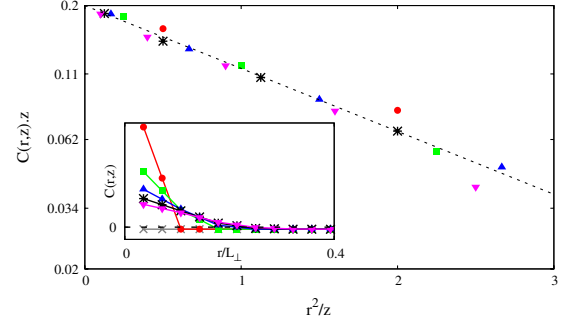

FIG. 3 (color online). Main panel: Behavior of $z \cdot C(\mathbf{r}, z)$ vs r^2/z, on a semilog scale for $z = 0$ (×), 2 (●), 4 (■), 6 (▲), 8 (+), 10 (▼). Dashed line shows behavior expected from Eq. (5). The system size is $L_\perp = 14$ and $L_z = 196$. Inset: Same data plotted as $C(\mathbf{r}, z)$ vs $r/L_\perp$ on a linear scale, showing that correlations vanish within (001) planes.

and treating $\mathcal{H}_Q$ using harmonic spin wave theory. Taking z and **r** to denote distances along the [001] direction and in the (001) plane, respectively, with ρ a microscopic length, two-point correlations at T_c are

$$C(\mathbf{r}, z) \propto \frac{1}{z} \exp\left(-\frac{|\mathbf{r}|^2}{\rho z}\right). \qquad (5)$$

This form reflects the string autocorrelations present in a random walk in two dimensions with propagation time z, and agrees well with results from simulations, as shown in Fig. 3. It is due to a fine tuned cancellation between the energy cost and entropy gain of an increase in the number of strings at T_c. Because of this cancellation, effective interactions between strings vanish [17].

A further consequence of this cancellation is that the surface tension between domains vanishes and the domain wall width diverges, as T_c is approached from below. We investigate this phenomenon in simulations by using weak, position-dependent magnetic fields to induce two domains with the interfaces between them lying on average in the x-z plane. Results are shown in Fig. 4. At T_c^- the magnetization profile $M(y)$ is a function only of $y/L_\perp$. Below T_c a mean field treatment of $\mathcal{H}_Q$ gives a domain wall width $\ell_w^{-1} \propto \sqrt{t} \equiv (1 - T/T_c)^{1/2}$: this is confirmed in Fig. 4, up
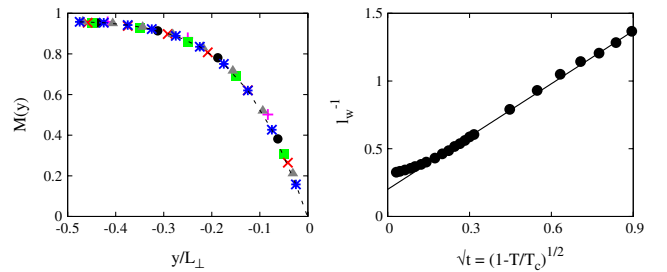

FIG. 4 (color online). Left: Magnetization profile vs $y/L_\perp$ at $T = 0.999T_c$ for $L_\perp = \{6, 8, 10, 12, 16, 20\}$. Right: Domain wall width ℓ_w vs $\sqrt{t}$ for $L_\perp = 20$. The straight line is a guide to the eye. All samples have $L_z = L_\perp^2$.
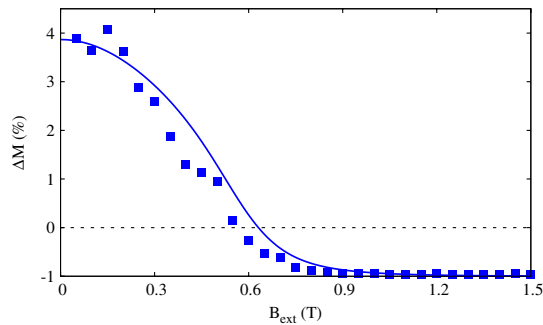
FIG. 5 (color online). Percentage change in magnetization measured under uniaxial pressure of 10.5 kbar, $M(P, B)$, compared to that at atmospheric pressure, $M(0, B)$, at $T = 1.7$ K as a function of applied field B_{ext} along the [001] axis ($\blacksquare$ extracted from [27]). The solid line is our best theoretical fit.

to a constant vanishing in the thermodynamic limit. The broad domain walls provide further evidence that we have a critical, rather than a first-order transition, and may be detectable using small angle neutron scattering.

The natural way to lift the degeneracy as required in a magnetic compound is to apply uniaxial pressure along the [001] axis of a single crystal. We need δ positive. Within the nearest neighbor approximation the effective coupling has two contributions, one from the long-range dipolar interactions [12,13,26], the other due to superexchange. While a uniaxial compression along [001] increases the former, the change of the latter is less obvious as it depends on the evolution of orbital overlaps.

Results from the one experiment so far performed on $Dy_2Ti_2O_7$ under pressure [27] suggest that the effective coupling is indeed modified so that $\delta > 0$. Pressure causes a 4% increase in M at small field, but a 1% decrease at high field (Fig. 5). The increase in the zero field susceptibility is consistent with the lifting of the degeneracy in favor of the states with magnetization along the field axis. The reduction of the saturated moment is expected when the crystal is squeezed along [001] because of the easy axes tilt away from [001].

We calculate the magnetization, $M(\delta, B, T)$, using a Husimi tree approximation for $Dy_2Ti_2O_7$: as we are above the upper critical dimension, this should be extremely accurate [17]. We estimate δ by comparing $M(\delta, B, T)$ to the data and fitting to the high field moment. The demagnetization effects are accounted for by modeling the sample as a prolate ellipsoid with major axes given by the dimensions of the approximately rectangular parallelepiped specimen. For the interaction parameter of $Dy_2Ti_2O_7$ [28], the best fit, shown in Fig. 5, yields $T_c = \frac{4\delta}{3\ln 2} \sim 200$ mK.

Whereas this temperature is comfortably within reach of cryogenics, the dynamics of spin ice slows down greatly below $T_f \sim 600$ mK, as activated ice-rule violating defects disappear. Their presence thus appears indispensable in practice, even though they lead to a more standard

second-order phase transition in the three-dimensional Ising universality class [17,20]. The width of its critical region, however, vanishes with defect concentration. One should thus aim at the lowest dynamically accessible transition temperatures, with the target $T_c \sim 600$ mK requiring a strain only 3 times larger than in existing experiments [27]. We hope our work will stimulate further experimental efforts to realize this unusual transition.

[1] C. L. Henley, Ann. Rev. Condens. Matter Phys. **1**, 179 (2010).
[2] F. Alet *et al.*, Phys. Rev. Lett. **97**, 030403 (2006).
[3] T. S. Pickles, T. E. Saunders, and J. T. Chalker, Europhys. Lett. **84**, 36 002 (2008).
[4] G. Chen *et al.*, Phys. Rev. B **80**, 045112 (2009).
[5] L. D. C. Jaubert *et al.*, Phys. Rev. Lett. **100**, 067207 (2008).
[6] I. Mirebeau *et al.*, Nature (London) **420**, 54 (2002).
[7] I. Mirebeau *et al.*, Phys. Rev. B **74**, 174414 (2006).
[8] M. E. Lines and A. M. Glass, *Principles and Applications of Ferroelectrics and Related Materials* (Clarendon, Oxford, 1977).
[9] J. C. Slater, J. Chem. Phys. **9**, 16 (1941).
[10] E. H. Lieb, Phys. Rev. Lett. **19**, 108 (1967).
[11] M. J. Harris *et al.*, Phys. Rev. Lett. **79**, 2554 (1997).
[12] M. J. P. Gingras and B. C. den Hertog, Can. J. Phys. **79**, 1339 (2001).
[13] S. V. Isakov, R. Moessner, and S. L. Sondhi, Phys. Rev. Lett. **95**, 217201 (2005).
[14] S. V. Isakov *et al.*, Phys. Rev. Lett. **93**, 167204 (2004).
[15] C. L. Henley, Phys. Rev. B **71**, 014424 (2005).
[16] S. V. Isakov *et al.*, Phys. Rev. B **70**, 104418 (2004).
[17] L. D. C. Jaubert, Ph. D. thesis, École Normale Supérieure de Lyon, 2009, http://hal.archives-ouvertes.fr/docs/00/46/29/70/PDF/Thesis.pdf.
[18] K. Binder, Rep. Prog. Phys. **50**, 783 (1987).
[19] H. Takahasi, Proc. Phys. Math. Soc. Jpn. **23**, 1069 (1941).
[20] Y. Takagi, J. Phys. Soc. Jpn. **3**, 273 (1948).
[21] J. F. Nagle, Commun. Math. Phys. **13**, 62 (1969).
[22] J. D. Shore and D. J. Bukman, Phys. Rev. Lett. **72**, 604 (1994).
[23] L. Benguigui, Phys. Rev. B **16**, 1266 (1977).
[24] R. J. Baxter, *Exactly Solved Models in Statistical Mechanics* (Dover Publications, Mineola, 2007), Chap. 8.
[25] S. Powell and J. T. Chalker, Phys. Rev. B **78**, 024422 (2008).
[26] R. Siddharthan *et al.*, Phys. Rev. Lett. **83**, 1854 (1999).
[27] M. Mito *et al.*, J. Magn. Magn. Mater. **310**, e432 (2007).
[28] B. C. den Hertog and M. J. P. Gingras, Phys. Rev. Lett. **84**, 3430 (2000).